DOI: 10.1534/genetics.107.072280

In Vivo Functional Specificity and Homeostasis of Drosophila 14-3-3 Proteins

Summer F. Acevedo,[1,2] K. Kirki Tsigkari,[1] Sofia Grammenoudi and Efthimios M. C. Skoulakis[3]

Institute of Molecular Biology and Genetics, Biomedical Sciences Research Centre "Alexander Fleming," 16672 Vari, Greece

Manuscript received February 19, 2007
Accepted for publication July 5, 2007

ABSTRACT

The functional specialization or redundancy of the ubiquitous 14-3-3 proteins constitutes a fundamental question in their biology and stems from their highly conserved structure and multiplicity of coexpressed isotypes. We address this question *in vivo* using mutations in the two Drosophila 14-3-3 genes, *leonardo* (*14-3-3ζ*) and *D14-3-3ε*. We demonstrate that D14-3-3ε is essential for embryonic hatching. Nevertheless, *D14-3-3ε* null homozygotes survive because they upregulate transcripts encoding the LEOII isoform at the time of hatching, compensating D14-3-3ε loss. This novel homeostatic response explains the reported functional redundancy of the Drosophila 14-3-3 isotypes and survival of *D14-3-3ε* mutants. The response appears unidirectional, as D14-3-3ε elevation upon LEO loss was not observed and elevation of *leo* transcripts was stage and tissue specific. In contrast, LEO levels are not changed in the wing disks, resulting in the aberrant wing veins characterizing *D14-3-3ε* mutants. Nevertheless, conditional overexpression of LEOI, but not of LEOII, in the wing disk can partially rescue the venation deficits. Thus, excess of a particular LEO isoform can functionally compensate for D14-3-3ε loss in a cellular-context-specific manner. These results demonstrate functional differences both among Drosophila 14-3-3 proteins and between the two LEO isoforms *in vivo*, which likely underlie differential dimer affinities toward 14-3-3 targets.

A fundamental issue concerning members of highly conserved protein families is the extent to which they are functionally redundant or exhibit specialized biological functions. The 14-3-3 proteins compose a highly conserved family of acidic molecules present in all eukaryotes (Aitken 1995; Wang and Shakes 1996; Rosenquist *et al.* 2000). 14-3-3's share a common structure composed of nine antiparallel α-helices forming a horseshoe shape with a negatively charged interior surface (Fu *et al.* 2000; Tzivion *et al.* 2001; Aitken *et al.* 2002; Bridges and Moorehead 2005; Van Heudsen 2005; Coblitz *et al.* 2006). Interactions among particular amino acids in the first helix, with ones in helix 2 and helix 3 of another monomer, promote dimerization (Luo *et al.* 1995; Xiao *et al.* 1995; Fu *et al.* 2000; Van Heudsen 2005). Dimerization generates a tandem binding surface, which can simultaneously bind to one or two sites on one target protein or to sites on two different client molecules. The dimers bind clients containing phosphoserine- or phosphothreonine-containing motifs via highly conserved amino acids within the groove (Muslin *et al.* 1996; Yaffe and Elia 2001; Tzivion and Avruch 2002). 14-3-3 proteins can also bind targets with surfaces outside the conserved phosphopeptide-binding cleft (Benton *et al.* 2002; Wilker *et al.* 2005). 14-3-3 binding may allosterically stabilize conformational changes, leading to activation or deactivation of the target or to interaction between two proteins (Yaffe 2002). Furthermore, 14-3-3 binding may mask or expose interaction sites, often leading to changes in the subcellular localization of client proteins (Van Hemert *et al.* 2001; Aitken *et al.* 2002; Bridges and Moorehead 2005; Van Heudsen 2005).

An extraordinary feature of this protein family is the high sequence conservation among isotypes, characterized by long stretches of invariant amino acids (Wang and Shakes 1996; Gardino *et al.* 2006), suggesting functional redundancy. However, despite this extensive sequence identity, multiple 14-3-3 proteins exist in metazoans, indicating at least some functional specificity. Vertebrates contain seven distinct protein isotypes, β, ε, ζ, γ, η, θ, and σ (Aitken *et al.* 1995). In vertebrate brains where these proteins are highly abundant, there is some specificity in isotype distribution, but generally 14-3-3's are expressed in complex overlapping patterns (Martin *et al.* 1994; Baxter *et al.* 2002). In addition, multiple heterodimers are possible in tissues that contain more than one isotype (Jones *et al.* 1995). It is unclear whether the presence of multiple highly similar proteins with overlapping distribution reflects functional differences among them or represents a mechanism to ensure that ample functionally redundant 14-3-3's are available to mediate the multiple essential cellular functions that require them (Van Heudsen 2005). Thus, the question of 14-3-3 functional specificity *in vivo* is fundamental in

[1]These authors contributed equally to this work.

[2]*Present address:* Oregon Health Sciences University, Behavioral Neuroscience L-470, 3181 SW Sam Jackson Park Rd., Portland, OR 97239.

[3]*Corresponding author:* Institute of Molecular Biology and Genetics, Biomedical Sciences Research Centre "Alexander Fleming," 34 Fleming Str., 16672 Vari, Greece. E-mail: skoulakis@fleming.gr

understanding their biology. The highly overlapping isotype distribution in vertebrate models hinders systematic investigation of this question.

To address the issue of functional specificity *in vivo*, we used *Drosophila melanogaster*, which offers a simple, but representative, genetically tractable metazoan system. It is simple because it contains only two 14-3-3 genes, an ortholog of the mammalian *14-3-3ζ* (88% identity) *leonardo* and an ortholog of the ϵ isotype, *D14-3-3ϵ* (Skoulakis and Davis 1998). It is representative because the two fly genes belong to the two different 14-3-3 conservation groups (Wang and Shakes 1996; Skoulakis and Davis 1998). *leonardo* encodes two nearly identical protein isoforms (LEO I and LEO II) via alternative splicing of the primary transcript (Kockel *et al.* 1997; Philip *et al.* 2001), with modest tissue specificity (Philip *et al.* 2001). In contrast, *D14-3-3ϵ* encodes a single protein (Chang and Rubin 1997), apparently present in all developmental stages and tissues examined with only slight enrichment in the adult brain (Tien *et al.* 1999; Philip *et al.* 2001).

Maternal LEO is required for normal chromosome separation during syncytial mitoses, whereas D14-3-3ϵ appears required to time them, suggesting distinct functions for the two 14-3-3's in the single-celled syncytial embryo (Su *et al.* 2001). Maternal LEO is also essential for early Raf-dependent decisions that pattern the embryo (Li *et al.* 1997). Zygotic *leo* loss-of-function mutants exhibit functional impairments of their embryonic and adult nervous system (Skoulakis and Davis 1996; Broadie *et al.* 1997; Philip *et al.* 2001). D14-3-3ϵ functions in photoreceptor formation and appears involved in development of the wing (Chang and Rubin 1997), but whether it is important for the function of the nervous system is unknown. LEO and D14-3-3ϵ appear at least partially redundant for photoreceptor formation (Karim *et al.* 1996; Chang and Rubin 1997). Furthermore, LEO and D14-3-3ϵ have been reported to function redundantly in anterior–posterior axis formation of the developing oocyte (Benton *et al.* 2002) and follicle cell polarity (Benton and St Johnston 2003).

Nevertheless, three reasons motivated a systematic investigation of potential functional specificity of the two Drosophila 14-3-3 isotypes by searching for isotype-specific phenotypes. First, studies to date used a transposon allele of D14-3-3ϵ (j2B10), which may not be a null allele. In fact, although *D14-3-3ϵ* has been reported dispensable for viability (Chang and Rubin 1997), a lethal deficiency uncovering this gene was used to show its involvement in Raf-mediated developmental processes in the embryo (Li *et al.* 2000). Second, *leo* mutations are homozygous lethal, suggesting that D14-3-3ϵ cannot functionally compensate for its loss, although LEO was suggested to at least partially compensate for the lack of D14-3-3ϵ in embryonic development (Chang and Rubin 1997). Third, the dynamic expression pattern of 14-3-3's during embryonic development and larval and adult nervous systems (Skoulakis and Davis 1996; Tien *et al.* 1999; Philip *et al.* 2001) suggested involvement in additional processes other than photoreceptor and oocyte development, which may specifically require one but not the other. Our results demonstrate 14-3-3-isotype-specific functions and a tissue- and temporal-specific transcriptional mechanism to compensate for loss of D14-3-3ϵ and suggest dynamic temporal and spatial interactions of the two 14-3-3 isotypes.

MATERIALS AND METHODS

Drosophila culture and strains: Drosophila were cultured in standard wheat–flour–sugar food supplemented with soy flour and $CaCl_2$ at 21°–23°, unless specified otherwise. The *D14-3-3ϵ$^{l(3)j2B10}$* mutant allele, which contains a P-transposon in intron 1 of the gene, has been described previously (Chang and Rubin 1997). Alleles *D14-3-3ϵ^{ex5}*, *D14-3-3ϵ^{ex4}*, and *D14-3-3ϵ^{ex24}* generated by mobilization of the transposon in *D14-3-3ϵ$^{l(3)j2B10}$* were a kind gift of Henry Chang and G. Rubin. The genetic background of these alleles was normalized using balancer chromosomes in a Cantonized *w^{1118}* background for *D14-3-3ϵ^{ex5}*, *D14-3-3ϵ^{ex4}*, and *D14-3-3ϵ^{ex24}*. In contrast, free recombination for six generations following the transposon-borne *w^{+}* as a selectable marker was allowed for *D14-3-3ϵ$^{l(3)j2B10}$*. Allelism was assessed by complementation tests of alleles normalized over the balancer with *D14-3-3ϵ$^{l(3)j2B10}$* recovered after normalization. The lethal *leo^{12X}* and *leo^{P1188}* alleles have been described previously (Broadie *et al.* 1997; Philip *et al.* 2001) and were normalized to the Cantonized *w^{1118}* genetic backround using balancer chromosomes.

Complementation tests for viability and wing cross-vein deficits were performed by crossing parents of the appropriate genotypes *en masse* and scoring the progeny of multiple such crosses per genotype. Viability was measured as the percentage of mutant homozygotes recovered from a cross of balanced parents, relative to the expected number if the homozygotes were fully viable. The expected number of homozygotes, if fully viable, was estimated as one-third of the total progeny recovered because homozygotes for the balancer chromosomes die as embryos. To rescue lethality with heat-shock (HS)-inducible transgenes, crosses were performed and animals were raised to adulthood in programmable cycling incubators (Labline) as described (Philip *et al.* 2001) or at constant 18° and 23°. Rescue for viability or cross-vein deficits was calculated as the percentage of expected homozygous individuals that increased upon transgene expression over that obtained from the same strain in the absence of transgene [(% viable induced) − (% viable baseline)/(100 − % viable baseline)]. Cross-vein deficit rescue was scored similarly. Each cross was repeated minimally four independent times and the data were pooled.

To determine the lethal phase of null homozygotes, embryos were collected from *D14-3-3ϵ$^{l(3)j2B10}$/TM3SerGFP* and *D14-3-3ϵ^{ex4}/TM3SerGFP* flies and manually separated into green fluorescent protein (GFP) fluorescence negative (homozygous mutant) and GFP fluorescence positive. Homozygotes for the balancers were avoided on the basis of their much more intense fluorescence. After hatching, they were monitored in separate food vials until emergence of adult flies at which time their genotype was verified again on the basis of adult visible markers.

The *hsleoI*, *hsleoII*, and *UAS-mycD14-3-3ϵ* transgenic strains have been described before (Philip *et al.* 2001; Chen *et al.* 2003). To generate *hsD14-3-3ϵ*, the entire *D14-3-3ϵ* cDNA (Chang and Rubin 1997) including the 3′ untranslated region was placed

into the *P{CaSpeRHS}* vector (Bourgouin *et al.* 1992) and multiple transformant lines on different chromosomes, were obtained. Insertions on the third chromosome were selected and recombined onto the *D14-3-3ε$^{l(3)j2B10}$*- and *D14-3-3ε^{ex4}*-bearing chromosomes with standard crosses. To generate *UASleoI* and *UASleoII*, the entire *leo* open reading frame was inserted in pUAST (Brand and Perrimon 1993) and multiple transformant lines were obtained. Again, insertions on the third chromosome were selected and recombined onto the *D14-3-3ε$^{l(3)j2B10}$*- and *D14-3-3ε^{ex4}*-bearing chromosomes.

Immunohistochemistry: Embryos were collected on apple juice plates, dechorionated, and fixed in 43.2 mm HEPES, 0.96 mm MgSO4, 0.48 mm EGTA, pH 6.9, 1.6% formaldehyde in 59% heptane, followed by rinses in methanol, 5% EGTA. The embryos were rehydrated to BBT (140 mm NaCl, 2.7 mm KCl, 4.3 mm Na_2HPO_4, 1.4 mm KH_2PO_4, pH 7.3, 0.1% Tween-20, 1%, bovine serum albumin) and blocked for 1 hr in BBT-250 (BBT, 250 mm NaCl), 10% normal goat serum. Incubation with primary antibodies in 5% normal goat serum BBT-250 was as follows: chicken anti-D14-3-3ε, 1:3000; mAb-22c10, 1:2000 [Developmental Hybridoma Studies Bank (DSHB), University of Iowa, Iowa City, IA]; mAb anti-FASIII, 1:10 (7G10-DSHB); mAb anti-NEUROTACTIN, 1:200 (BP106-DSHB); and rabbit polyclonal anti-MEF2, 1:1000 (Nguyen and Xu 1998). Fluorescent (Molecular Probes, Eugene, OR) and HRP-conjugated (Jackson Immunochemicals) secondary antibodies were used at 1:2000. Homozygous embryos were identified on the basis of their lack of signal against the balancer-chromosome-borne GFP. Embryos homozygous for the balancer were avoided on the basis of their abnormal appearance. Anti-GFP antibodies were a rabbit polyclonal, 1:40 (Santa Cruz), and a mAb 1:2000 (Molecular Probes). Images were captured on a Zeiss Axiovert 200 microscope.

Wing mounting: Wings were dissected in 95% ethanol and placed in xylene for 10 min, washed twice with ethanol, and mounted in Canada balsam (C-1795, Sigma, St. Louis). Images were captured on a Zeiss Axiovert 35 microscope using a ×20 objective lens.

Western blot analysis: To obtain extracts from homozygous embryos, GFP fluorescence-negative embryos were hand selected from eggs laid by *D14-3-3ε$^{l(3)j2B10}$/TM3SerGFP* and *D14-3-3ε$^{l(3)j2B10}$/TM3SerGFP* parents. Sibling GFP fluorescence-positive heterozygous embryos were selected as controls because they fluoresced and appeared normal. Homozygotes for the balancers were not used and were identified on the basis of their more intense fluorescence and abnormal appearance relative to heterozygotes. The fidelity of the embryonic genotype based on the above criteria was verified on similarly selected embryos by immunohistochemistry. Single flies or an embryo equivalent to three fly heads per lane from control and mutant animals was homogenized in 10 μl of modified radioimmunoprecipitation assay buffer as previously described (Philip *et al.* 2001). Blots were rabbit anti-LEO, 1:40,000; chicken anti-D14-3-3ε, 1:5000; mAb antitubulin, 1:300 (E7-DSHB); mAb antisyntaxin, 1:500 (8C3-DSHB); and anti-cMyc, 1:200 (9E10-DSHB). Secondary antibodies were used 1:15,000 for anti-rabbit HRP, 1:5000 for anti-chicken HRP, and 1:5000 for anti-mouse HRP and the results were visualized with enhanced chemiluminescence (Pierce, Rockford, IL). The results of at least three independent experiments utilizing different extract preparations were quantified densitometrically and analyzed statistically.

The chicken anti-D14-3-3ε antibody was generated by immunizing hens (Charles River Laboratories) with a his-tagged, bacterially expressed fragment of the D14-3-3ε protein containing the amino-terminal 130 amino acids. IgY was purified from eggs using standard procedures (Charles River Laboratories). Eggs from two different hens yielded antibodies with nearly identical properties, but one of them was used throughout these experiments. The specificity of the anti-D14-3-3ε antibodies was tested against recombinant D14-3-3ε and D14-3-3ζ (LEO) (Skoulakis and Davis 1996) and fly lysates.

Reverse transcription–polymerase chain reaction analysis and quantitative PCR: Hand-selected embryos and larval wing disk and brain samples were prepared and reverse transcription–polymerase chain reaction (RT–PCR) reactions with *leoI*, *leo II*, and *D14-3-3ε* primers were performed as previously described (Philip *et al.* 2001). As an internal control, forward and reverse *act5C* primers were used to quantify the relative amount of RNA in each sample. To identify *hsleoI*, the *leoI* forward primer was used with *SV40*-specific reverse primer and, for *hsleoII*, the *leoII* forward primer was used with a *hsp70*-specific reverse primer. For the quantitative RT–PCR experiments, newly hatched larvae were hand selected on the basis of their lack of GFP fluorescence, and 1 μg of RNA (Philip *et al.* 2001) was subjected to reverse transcription; the product was diluted 1:100 and 4 μl were used per PCR reaction. Each reverse transcription was sampled four times per PCR run and five independent experiments were performed. *leoI*, *leoII*, *D14-3-3ε*, and *act5C* primers were used as described above. A calibration curve was constructed for each run and used to fit the values (Pfaffl 2001). Relative quantification was performed using the MJ Opticon Monitor Analysis software (v3.1), with the relative quantification method ΔΔCt ("Guide to Performing Relative Quantification of Gene Expression using Real-Time Quantitative PCR," Applied Biosystems, Foster City, CA).

Statistical analysis: Untransformed data from densitometric quantification of protein amounts and the results of cell-counting experiments and complementation tests were analyzed using the JMP3.1 statistical software package (SAS Institute, Cary, NC). Following initial ANOVA, the data were analyzed by Student's *t*-tests or planned comparisons to a control (Dunnett's test) where appropriate.

RESULTS

Loss of *D14-3-3ε* compromises viability: To unequivocally determine whether D14-3-3ε is required for viability, we sought to identify null alleles by characterizing derivatives of transposon mobilization from *D14-3-3ε$^{l(3)j2B10}$* (Chang and Rubin 1997). Southern analysis (not shown) demonstrated that *D14-3-3ε^{ex4}* harbors a small deletion removing the first exon and part of the first intron of the gene. Allele *D14-3-3ε^{ex24}* results from a large deletion (>10 kb) extending beyond the *D14-3-3ε* coding region and likely encompasses at least part of the CG7156 and CG18598 transcription units on either side of the gene (Figure 1A). In contrast, excision of the transposon in *D14-3-3ε^{ex5}* did not result in obvious DNA rearrangements. Furthermore, genomic PCR and high-resolution acrylamide electrophoresis of the DNA flanking the transposon insertion from *D14-3-3ε^{ex5}* homozygotes did not indicate size differences from the *w^{1118}* control (not shown). These results, in addition to the full viability of *D14-3-3ε^{ex5}* homozygotes (Table 1) and the lack of the visible phenotypes exhibited by *D14-3-3ε$^{l(3)j2B10}$*, *D14-3-3ε^{ex4}* homozygotes, suggest that *D14-3-3ε^{ex5}* represents a precise excision allele (Figure 1A). In accord with these results, D14-3-3ε protein was detected in *D14-3-3ε^{ex5}* homozygotes, but it was undetectable in *D14-3-3ε$^{l(3)j2B10}$*,

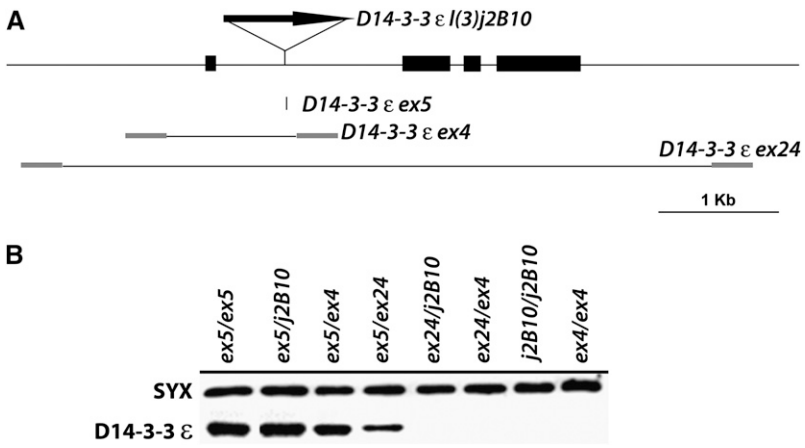

FIGURE 1.—*D14-3-3ϵ* mutations and their effects on protein accumulation. (A) The genomic region and mutations of the *D14-3-3ϵ* gene. Exons are represented by solid boxes and introns and surrounding nontranscribed regions by lines. The *P*-element insertion in intron 1 is indicated by the arrow. The deleted DNA in *D14-3-3ϵ^{ex4}* and *D14-3-3ϵ^{ex24}* is indicated by the lines flanked by shaded boxes representing regions of uncertainty at the ends of the deficiencies. A perpendicular line indicates the precise excision of the j2B10 transposon in the revertant allele *D14-3-3ϵ^{ex5}*. (B) Mutant homozygotes and heteroallelic combinations yield adult animals lacking D14-3-3ϵ protein demonstrated by semiquantitative Western blot analysis of whole-animal lysates of the indicated genotypes. The neuronal protein syntaxin (SYX) was used to control for the amount loaded per lane. *ex5* stands for *D14-3-3ϵ^{ex5}*, *j2B10* for *D14-3-3ϵ$^{l(3)j2B10}$*, *ex4* for *D14-3-3ϵ^{ex4}*, and *ex24* for *D14-3-3ϵ^{ex24}*.

D14-3-3ϵ^{ex4} homozygotes and heteroallelics with *D14-3-3ϵ^{ex24}* (Figure 1B). Therefore, by molecular criteria, *D14-3-3ϵ^{ex4}* and *D14-3-3ϵ^{ex24}* represent null alleles. Although *D14-3-3ϵ$^{l(3)j2B10}$* lacks detectable protein in these assays, we consider it a strong hypomorph on the basis of the genetic data below.

Although null, homozygotes for the *D14-3-3ϵ$^{l(3)j2B10}$* and *D14-3-3ϵ^{ex4}* alleles were recovered with lower frequency than expected if fully viable. This observation and the fact that the original *D14-3-3ϵ$^{l(3)j2B10}$* chromosome was associated with a lethal mutation (CHANG and RUBIN 1997) motivated us to perform complementation tests to determine whether *D14-3-3ϵ* is dispensable for viability. To avoid complications, chromosomes bearing *D14-3-3ϵ* mutations were introduced into our isogenized *w^{1118}* background (see MATERIALS AND METHODS). Even in the normalized genetic background, a fraction of the expected *D14-3-3ϵ$^{l(3)j2B10}$* and *D14-3-3ϵ^{ex4}* homozygotes and heteroallelics were recovered (Table 1). Thus, the reduced viability phenotype is fully recessive, maps exclusively to mutations in the *D14-3-3ϵ* gene, and does not appear to be modified by extragenic mutations. Although protein was not detectable in *D14-3-3ϵ$^{l(3)j2B10}$* adult homozygotes, the allele appears to be hypomorphic because of the larger number of *D14-3-3ϵ$^{l(3)j2B10}$* homozygotes and *D14-3-3ϵ$^{l(3)j2B10}$/D14-3-3ϵ^{ex4}* heteroallelics recovered compared to *D14-3-3ϵ^{ex4}* homozygotes. Because homozygotes were never recovered, the *D14-3-3ϵ^{ex24}* deficiency appears to disrupt neighboring gene(s), as suggested by the molecular data (Figure 1), and was excluded from further analyses.

The reduction in the number of *D14-3-3ϵ^{ex4}* and *D14-3-3ϵ$^{l(3)j2B10}$* homozygotes was fully rescued by induction of *hsD14-3-3ϵ* transgenes (Table 2). We used two independent transgenic lines, the high-expressing *hsD14-3-3ϵ^{H}* and lower-expressing *hsD14-3-3ϵ^{L}* (supplemental Figure 1 at http://www.genetics.org/supplemental/) with similar results. Lower, yet significant rescue, especially for *D14-3-3ϵ$^{l(3)j2B10}$* homozygotes, was obtained when the animals were raised at 23°, a consequence of high basal transgene expression (supplemental Figure 1 at http://www.genetics.org/supplemental/). For transgene-carrying mutant animals raised at 18°, the number of homozygotes was similar to that obtained from mutants without the transgene. These results confirm that D14-3-3ϵ loss results in significantly reduced viability. Given the "leakiness" of the transgenes, to verify that it was indeed elevation of the transgenic protein that rescued the phenotype, we placed *UAS-mycD14-3-3ϵ* transgenes into *D14-3-3ϵ^{ex4}* and *D14-3-3ϵ$^{l(3)j2B10}$* mutant backgrounds. Ubiquitous expression of *UAS-mycD14-3-3ϵ* transgenes with the *tubPGal4* driver fully rescued the lethality of *D14-3-3ϵ^{ex4}* (Table 2) and *D14-3-3ϵ$^{l(3)j2B10}$* homozygotes (not shown).

These results indicate that loss of D14-3-3ϵ results in significantly reduced survival (58% of *D14-3-3ϵ^{ex4}*

TABLE 1

Complementation for viability of *D14-3-3ϵ* mutants

Genotype	% viable	*n*
D14-3-3ϵ^{ex5}/D14-3-3ϵ^{ex5}	100	550
D14-3-3ϵ^{ex5}/D14-3-3ϵ$^{l(3)j2B10}$	100	413
D14-3-3ϵ^{ex5}/D14-3-3ϵ^{ex4}	100	546
D14-3-3ϵ^{ex5}/D14-3-3ϵ^{ex24}	100	660
D14-3-3ϵ$^{l(3)j2B10}$/D14-3-3ϵ$^{l(3)j2B10}$	75	645
D14-3-3ϵ$^{l(3)j2B10}$/D14-3-3ϵ^{ex4}	71	510
D14-3-3ϵ$^{l(3)j2B10}$/D14-3-3ϵ^{ex24}	61	510
D14-3-3ϵ^{ex4}/D14-3-3ϵ^{ex4}	42	495
D14-3-3ϵ^{ex4}/D14-3-3ϵ^{ex24}	39	684
D14-3-3ϵ^{ex24}/D14-3-3ϵ^{ex24}	0	650

D14-3-3ε^{ex4} and *D14-3-3ε^{ex24}* are novel mutant alleles of *D14-3-3ε*. Viability was calculated as the fraction of adults of each genotype recovered from crosses of balanced individuals over that expected if the mutant homozygotes or heteroallelics were fully viable. *n* denotes the total number of flies scored per cross.

TABLE 2

Transgenic rescue of *D14-3-3ε* mutant lethality

Genotype	Temperature	% viable	% rescue	*n*
D14-3-3ε$^{l(3)j2B10}$/D14-3-3ε$^{l(3)j2B10}$	18°	75	—	645
D14-3-3ε$^{l(3)j2B10}$/D14-3-3ε$^{l(3)j2B10}$	23°	77	8	526
D14-3-3ε$^{l(3)j2B10}$/D14-3-3ε$^{l(3)j2B10}$	HS	78	12	522
D14-3-3ε$^{l(3)j2B10}$/D14-3-3ε$^{l(3)j2B10}$, hsD14-3-3ε	18°	74	—	462
D14-3-3ε$^{l(3)j2B10}$/D14-3-3ε$^{l(3)j2B10}$, hsD14-3-3ε	23°	81	27[a]	487
D14-3-3ε$^{l(3)j2B10}$/D14-3-3ε$^{l(3)j2B10}$, hsD14-3-3ε	HS	99	96.2[a]	508
D14-3-3ε^{ex4}/D14-3-3ε^{ex4}	18°	42	—	382
D14-3-3ε^{ex4}/D14-3-3ε^{ex4}	23°	45	5	411
D14-3-3ε^{ex4}/D14-3-3ε^{ex4}	HS	45	5	409
D14-3-3ε^{ex4}/D14-3-3ε^{ex4}, hsD14-3-3ε	18°	40	—	495
D14-3-3ε^{ex4}/D14-3-3ε^{ex4}, hsD14-3-3ε	23°	44	7	488
D14-3-3ε^{ex4}/D14-3-3ε^{ex4}, hsD14-3-3ε	HS	92	86.7[a]	488
D14-3-3ε^{ex4}, tubPGal4/D14-3-3ε^{ex4}	25°	39	—	245
UASmycD14-3-3ε^{L}/+ ; D14-3-3ε^{ex4}, tubPGal4/D14-3-3ε^{ex4}	25°	87	78.6[a]	568
UASmycD14-3-3ε^{H}/+ ; D14-3-3ε^{ex4}/D14-3-3ε^{ex4}	25°	42	5	268
UASmycD14-3-3ε^{H}/+ ; D14-3-3ε^{ex4}, tubPGal4/D14-3-3ε^{ex4}	25°	100	100[a]	592
elavGal4/+; UASmyc D14-3-3ε^{L}/+ ; D14-3-3ε^{ex4}/D14-3-3ε^{ex4}	25°	97	95[a]	812
+/+; UASmyc D14-3-3ε^{H}/+ ; D14-3-3ε^{ex4}/D14-3-3ε^{ex4}	25°	44	8.2	327
elavGal4/+; UASmyc D14-3-3ε^{H}/+ ; D14-3-3ε^{ex4}/D14-3-3ε^{ex4}	25°	100	100[a]	825

Transgenic reversal of *D14-3-3ε* homozygous mutant lethality. All transgenic strains and controls were grown under the three regimes indicated under "Temperature"—constant 18°, constant 23°, and HS conditions of constant 23° with three daily 30-min, 32° heat shocks. All Gal4 driven crosses were performed at constant 25°. Viability was calculated as the fraction of adults of each genotype recovered from crosses of balanced individuals over that expected if the mutant homozygotes were fully viable. "% rescue" was calculated as the percentage increase in mutant homozygotes carrying transgenes over the "baseline" number (denoted by "—") obtained at 18° for experiments employing HS-inducible transgenes. *n* denotes the total number of flies scored per cross. Significant rescue was not observed in the absence of the transgenes although a few more homozygotes were obtained under HS conditions.

[a] Significant rescue.

homozygotes die). Therefore, the protein is required for complete viability in contrast to previous reports suggesting that the gene is not essential (Chang and Rubin 1997). In contrast, null alleles of the Drosophila 14-3-3ζ gene *leonardo* are fully lethal when homozygous (Skoulakis and Davis 1996; Broadie *et al.* 1997).

Morphological characterization of *D14-3-3ε* homozygous mutant embryos: We examined the fate of homozygous embryos to determine when *D14-3-3ε* mutants die. They were identified because they lacked the fluorescence of the balancer-chromosome-borne GFP. Clearly, 100% of null embryos that hatched successfully proceeded to adulthood (Table 3), as their number [72% for *D14-3-3ε$^{(3)j2B10}$* and 40% for *D14-3-3ε^{ex4}*] reflected that of the adult homozygotes typically recovered. Therefore, D14-3-3ε does not appear to be required for vital functions in the larval and pupal stages, but it is critical at the time of hatching. In agreement, embryos that failed to hatch remained alive for an additional 6–12 hr as indicated by their occasional peristaltic movements and, if manually removed from the chorion, many survived to adulthood.

To determine whether null embryos failed to hatch because of developmental defects, we subjected them to immunohistochemical analysis. Most *D14-3-3ε* mutant embryos appeared smaller in size, but staining with anti-FASIII did not reveal gross morphological changes (Figure 2, A–D). Because we hypothesized that the inability to hatch could be a reflection of neuro-developmental deficits since both D14-3-3ε and LEO are abundant in this tissue (Skoulakis and Davis 1996; Tien *et al.* 1999), we

TABLE 3

Lethal phase of *D14-3-3ε* null homozygotes

Genotype	% hatching	% eclosed	*n*
D14-3-3ε$^{l(3)j2B10}$/TM3SerGFP	100	100	228
D14-3-3ε$^{l(3)j2B10}$/D14-3-3ε$^{l(3)j2B10}$	72	100	203
D14-3-3ε^{ex4}/TM3SerGFP	100	100	309
D14-3-3ε^{ex4}/D14-3-3ε^{ex4}	40	100	216

D14-3-3ε homozygous mutants die as embryos. The genotypes of the embryos were ascertained on the basis of the GFP fluorescence as described in materials and methods and verified upon eclosure of adults. "% hatching" indicates the percentage of embryos yielding larvae, while "% eclosed" denotes the percentage of hatched embryos that became adults. *n* denotes the total number of embryos assayed per genotype.

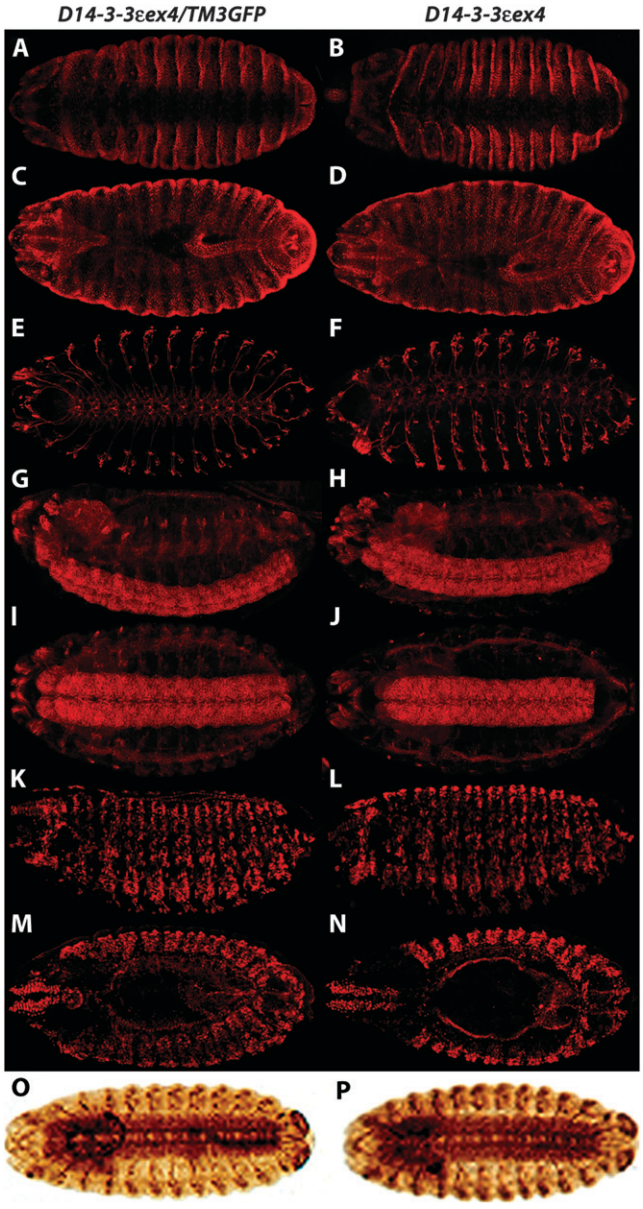

Figure 2.—Morphology of *D14-3-3ϵ* homozygous mutant embryos. Embryos (16–18 hr old) are shown. Anterior is to the left. The genotype ascertained by concurrent staining with anti-GFP (see materials and methods) is shown on top of the two columns. A and B are ventral views, while C and D are dorsal views of embryos stained with anti-FASIII. There were no obvious gross morphological defects. E and F are ventral views of control and mutant embryos, respectively, stained with mAb22c10, and not showing overall deficits in CNS and PNS morphology. This was further demonstrated in homozygotes that failed to hatch (P), compared to heterozygotes 20 hr post-egg laying (O). The CNS and, to a lesser degree, the PNS were also examined with anti-neurotactin. I and J are lateral views, while K and L are ventral views and, in agreement with E and F, do not exhibit obvious structural differences of the CNS (and PNS) in mutant homozygotes compared to their heterozygous siblings. Similar results were obtained with homozygous embryos that failed to hatch (not shown). K and L are lateral views and M and N are dorsal views of embryos stained with anti-MEF-2, which failed to reveal significant changes in the musculature of the mutants.

focused on the nervous system. Staining of $D14\text{-}3\text{-}3\epsilon^{ex4}$ homozygotes with mAb22c10 and anti-NEUROTACTIN did not reveal morphological changes in the central nervous system (CNS) and peripheral nervous system (PNS) (Figure 2, E–J) or in the musculature revealed by anti-MEF staining (Figure 2, K–N). To ascertain that we did not focus on embryos that appeared normal because they would be among ones that hatch successfully, embryos that failed to hatch 24–26 hr post-egg laying (PEL) were collected and stained with anti-FASIII and mAb22c10. These $D14\text{-}3\text{-}3\epsilon^{ex4}$ homozygotes appeared identical to controls as well (Figure 2, O and P). Similar results were obtained with $D14\text{-}3\text{-}3\epsilon^{l(3)j2B10}$ homozygotes (not shown). Therefore, lack of D14-3-3ϵ did not result in gross developmental aberrations and homozygotes died as apparently fully formed larvae.

To determine whether functional deficits of the nervous system, akin to those described for *leo* nulls (Broadie *et al.* 1997), result in the observed failure of *D14-3-3ϵ* mutant homozygotes to hatch, we targeted transgene expression to the nervous system. *UAS-mycD14-3-3ϵ* transgenes driven specifically in the nervous system with the *elavGal4* driver (Robinow and White 1988) were strikingly efficient at increasing the number of $D14\text{-}3\text{-}3\epsilon^{ex4}$ homozygotes recovered (Table 2). Thus, lethality of *D14-3-3ϵ* mutant homozygotes results from failure of the nervous system to support normal hatching and is consistent with the described preferential distribution of the protein in the CNS and PNS of late embryos (Tien *et al.* 1999).

Upregulation of LEO in D14-3-3ϵ mutant embryos: $D14\text{-}3\text{-}3\epsilon^{ex4}$ or $D14\text{-}3\text{-}3\epsilon^{l(3)j2B10}$ homozygotes were not recovered if the animals were also made heterozygous for a strong *leo* mutant allele (Chang and Rubin 1997; E. M. C. Skoulakis, unpublished results). This observation suggested that LEO may compensate for the loss of D14-3-3ϵ during embryonic development and this may be responsible for the recovery of homozygous mutants. To address this hypothesis, lysates from 18- to 20-hr-old homozygous embryos, hand selected on the basis of their lack of GFP fluorescence, were subjected to semiquantitative Western blot analysis. The representative results in Figure 3A and quantified in Figure 3B show that in homozygous null embryos there was a highly significant increase in the amount of LEO compared to that in sibling heterozygotes or control animals. Because we could not distinguish which of the embryos would hatch and survive, it was not possible to determine whether this increase characterized all embryos, homozygotes destined to die, or only potential survivors. If the latter is the case, then we underestimated the actual level of LEO in survivors because the lysates included embryos destined to die where this elevation may not occur.

To determine when this LEO elevation occurs, we examined lysates from tightly staged embryos. Mutant embryos were individually selected from half-hour egg collections, dechorionated, and visually inspected under the microscope to ascertain stage homogeneity before

preparation of lysates. We quantified LEO levels in later stages of embryogenesis relative to maternally provided protein (Li *et al.* 1997; Philip *et al.* 2001), which we found relatively invariable over many different experiments (not shown). Thus, compared to 1- to 3-hr control embryos, LEO levels were significantly higher in 22-hr *D14-3-3ε^{ex4}* homozygotes and nearly doubled during their 2-hr hatching delay (Figure 3, C and D). Similar results were obtained with *D14-3-3ε$^{l(3)j2B10}$* homozygotes. Therefore, elevation of LEO in *D14-3-3ε* null embryos occurs late in embryogenesis, particularly during the hatching delay exhibited by mutant homozygotes. These results are consistent with two notions. First, elevation of LEO in *D14-3-3ε* mutant homozygotes may be the reason a fraction hatches and represents a compensatory mechanism for the loss of D14-3-3ε. Alternatively, LEO elevation occurs in embryos unable to hatch and may represent a stress response that characterizes dying or dead embryos similar to the reported postmortem elevation of certain vertebrate 14-3-3 isotypes (Foundoulakis *et al.* 2001).

To investigate whether elevation of LEO was a consequence of increased transcription in *D14-3-3ε* mutants, we estimated the relative levels of the two *leo* transcripts by quantitative PCR. LEOI and LEOII differ by five amino acids encoded in the alternative, mutually exclusive exons 6 and 6′ (Philip *et al.* 2001). We used newly hatched homozygous mutant larvae for this quantification because, if detectable, it would indicate that *leo* elevation occurs in animals that hatch. The 50% reduction in *D14-3-3ε* transcripts in heterozygotes and the lack of transcripts in homozygous mutants were easily detectable with our experimental conditions (Figure 4A). In these animals, the level of *leoI* transcripts remained unchanged, but we detected a significant increase in the level of *leoII* mRNA in heterozygotes and *D14-3-3ε^{ex4}* homozygous mutant larvae. The *leo* gene contains two alternative 5′ untranslated exons (exon 1 and 1′). Whereas *leoI* transcripts appear to always utilize exon 1′, *leoII* transcripts contain either the distal exon 1′

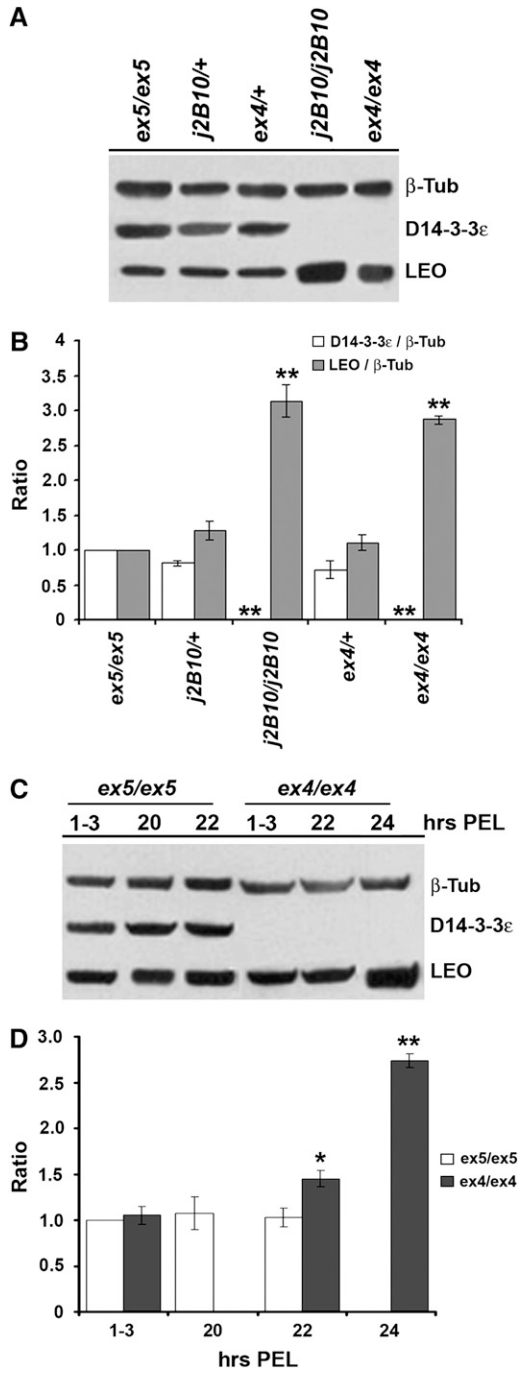

Figure 3.—Elevation of LEO in *D14-3-3ε* homozygous mutant embryos. (A) A representative blot of embryonic lysates used in acquisition of the data on B. The genotypes of the embryos whose lysates were blotted are indicated on top of the blot: *ex5/ex5* for *D14-3-3ε^{ex5}/D14-3-3ε^{ex5}*; *j2B10/+* for *D14-3-3ε$^{l(3)j2B10}$/D14-3-3ε^{ex5}*; *ex4/+* for *D14-3-3ε^{ex4}/D14-3-3ε^{ex5}*; *j2B10/j2B10* for *D14-3-3ε$^{l(3)j2B10}$/D14-3-3ε$^{l(3)j2B10}$*; and *ex4/ex4* for *D14-3-3ε^{ex4}/D14-3-3ε^{ex4}*. These abbreviations are used in A–D. β-Tub denotes β-tubulin, the protein used to normalize the lanes for the amount loaded. (B) The average ratios (± standard error of the mean or SEM) of the relative levels of LEO/β-Tub and D14-3-3ε/β-Tub is shown from four individual blots similar to the one displayed in A. Ratios are shown relative to those obtained from *D14-3-3ε^{ex5}* homozygotes, which were arbitrarily set to 1. The level of LEO accumulation was significantly higher (**$P < 0.001$) in *D14-3-3ε$^{l(3)j2B10}$* and *D14-3-3ε^{ex4}* homozygotes compared to *D14-3-3ε^{ex5}* controls. (C) A representative blot of embryonic lysates of the indicated genotypes prepared at the particular times PEL. The latest collection was at 24 hr for *D14-3-3ε^{ex4}* homozygotes because of their hatching delay, while the latest time point for control embryos was immediately before hatching at 22 hr. (D) The average ratio of relative levels of LEO/β-Tub ± SEM for *D14-3-3ε^{ex4}* homozygotes compared to *D14-3-3ε^{ex5}* controls estimated from three independent blots similar to the one shown in C. There is a highly significant increase (**$P < 0.001$) in the amount of LEO in *D14-3-3ε^{ex4}* homozygotes during their 2-hr hatching delay. A smaller increase (*$P < 0.05$) in *D14-3-3ε^{ex4}* homozygotes was detected at 22-hr PEL in comparison to *D14-3-3ε^{ex5}* controls of the same age. Samples from *D14-3-3ε^{ex4}* homozygotes were not collected at 20-hr PEL and control samples could not be collected at 24-hr PEL because the embryos had hatched to larvae.

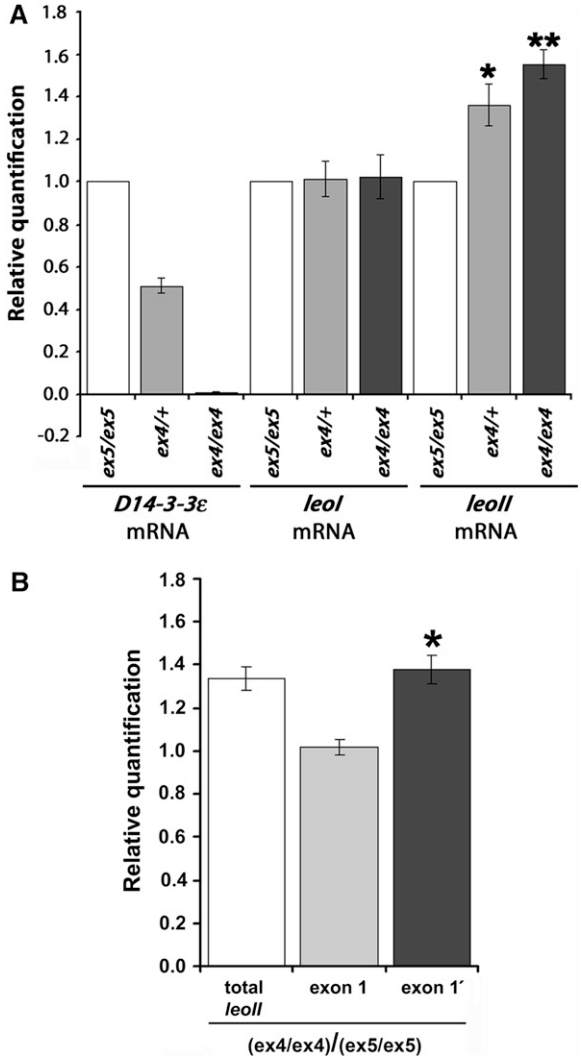

FIGURE 4.—Elevation of *leoII* transcripts in *D14-3-3*ϵ^{ex4} mutant homozygotes. (A) The ratios of *D14-3-3*ϵ/*act5C*, *leoI*/*act5C*, and *leoII*/*act5C* RT–PCR products in control animals were arbitrarily set to 1 (open bars) and their relative levels in *D14-3-3*ϵ^{ex4} heterozygotes (shaded bars) and homozygotes (solid bars) were determined. The mean ± SEM of five independent experiments is shown. *leoI* levels relative to those of *act5C* were not found significantly different in mutant heterozygotes and homozygotes. In contrast, the relative levels of *leoII* mRNAs were significantly higher than controls in both mutant heterozygotes ($*P < 0.01$) and homozygotes ($**P < 0.001$). (B) The ratios of *leoII* transcripts in *D14-3-3*ϵ^{ex4} homozygotes over those of control animals $[(ex^4/ex^4)/(ex^5/ex^5)]$ determined in experiments independent from those in A. Elevation of *leoII* in the mutants is detected because the ratio for "total *leoII*" is >1. Using primers specific to exon 1 and exon 1′, the levels of transcripts that include exon 1′ in the mutants were found significantly higher ($*P < 0.01$) than transcripts that include exon 1. The mean ± SEM of four independent experiments is shown.

or the proximal exon 1 (KOCKEL *et al.* 1997), suggesting differential use of promoters. We investigated whether both alternate exons are utilized in *D14-3-3*ϵ^{ex4} homozygotes to elevate *leoII* transcripts. However, the ratio of exon 1-containing transcripts in *D14-3-3*ϵ^{ex4} homozygotes to those present in control animals remained unchanged (1.015 ± 0.037). In contrast, the number of exon 1′-containing transcripts in the mutants was significantly higher (Figure 4B). This suggests that elevation of *leoII* transcripts in *D14-3-3*ϵ^{ex4} homozygotes involves increased utilization of the putative proximal promoter and differential inclusion of exon 1′ in these transcripts. These data strongly suggest that elevation of LEO protein levels are a consequence of upregulation of *leoII* transcripts. Since this is detected in mutant first instar larvae, the data suggest that elevation of *leoII* transcripts allows hatching and survival in the fraction of *D14-3-3*ϵ homozygotes where it occurs.

Conditional overexpression of *leo* transgenes rescues lethality of *D14-3-3*ϵ null homozygotes: To rigorously test the hypothesis that elevation of LEOII is the reason for hatching and survival of mutant homozygotes, *leoI* and *leoII* transgenes were recombined onto the chromosomes bearing the *D14-3-3*ϵ^{ex4} and *D14-3-3*$\epsilon^{l(3)j2B10}$ mutations. If endogenous LEOII elevation suffices for successful hatching of *D14-3-3*ϵ homozygotes, then further increasing the level of this protein should increase the number of homozygous mutant animals recovered. *hsleoI* and *hsleoII* transgenes exhibited leaky expression at 25°, but expression was higher after three daily inductions (HS) and undetectable if flies were kept at 18° (supplemental Figure 1 at http://www.genetics.org/supplemental/). Significantly, two independent insertions of a *hsleoII* trangene were able to conditionally increase (rescue) the number of *D14-3-3*ϵ^{ex4} and *D14-3-3*$\epsilon^{l(3)j2B10}$ homozygotes recovered (Table 4). In contrast, *hsleoI* transgenes rescued the phenotype only partially, despite the similarity in *hsleoI* and *hsleoII* transgene expression (supplemental Figure 1).

Importantly, when driven by the neuronal-specific Gal4 driver *elav*, *UASleoII* transgenes rescued fully and *UASleoI* partially, the lethality of *D14-3-3*ϵ^{ex4} homozygotes, consistent with the notion that they die because their nervous system is unable to support hatching (Table 4). This is not the result of differences in transgene expression levels, since independent *leoI* and *leoII* transgenes inducible by different means yielded similar outcomes. These data suggest that LEOII and, to a lesser degree, LEOI are functionally redundant with D14-3-3ϵ in the nervous system and confirm that LEOII elevation in a fraction of late *D14-3-3*ϵ mutant embryos allows them to hatch. Furthermore, the data indicate that, despite the minor, largely conservative differences (PHILIP *et al.* 2001), the two LEO isoforms are not equivalent in compensating for the lack of D14-3-3ϵ. Expression of *leo* transgenes in the nervous system is not ectopic, as LEO accumulates abundantly in this tissue (SKOULAKIS and DAVIS 1996; BROADIE *et al.* 1997).

The level of D14-3-3ϵ is not increased in homozygous *leo* null embryos: Is the level of one 14-3-3 isotype always elevated when the other is reduced during embryogenesis? Like null *D14-3-3*ϵ embryos, homozygotes

TABLE 4

Rescue of *D14-3-3ϵ* lethality with *leo* transgenes

Genotype	Temperature	% viable	% rescue	*n*
D14-3-3ϵ$^{l(3)j2B10}$/D14-3-3ϵ$^{l(3)j2B10}$	18°	75	—	645
D14-3-3ϵ$^{l(3)j2B10}$/D14-3-3ϵ$^{l(3)j2B10}$	23°	77	8	526
D14-3-3ϵ$^{l(3)j2B10}$/D14-3-3ϵ$^{l(3)j2B10}$	HS	78	12	522
D14-3-3ϵ$^{l(3)j2B10}$/D14-3-3ϵ$^{l(3)j2B10}$, hsleoI^{L}	18°	76	—	462
D14-3-3ϵ$^{l(3)j2B10}$/D14-3-3ϵ$^{l(3)j2B10}$, hsleoI^{L}	23°	84	33	455
D14-3-3ϵ$^{l(3)j2B10}$/D14-3-3ϵ$^{l(3)j2B10}$, hsleoI^{L}	HS	88	50	524
D14-3-3ϵ$^{l(3)j2B10}$/D14-3-3ϵ$^{l(3)j2B10}$, hsleoII^{L}	18°	78	—	442
D14-3-3ϵ$^{l(3)j2B10}$/D14-3-3ϵ$^{l(3)j2B10}$, hsleoII^{L}	23°	95	77[a]	492
D14-3-3ϵ$^{l(3)j2B10}$/D14-3-3ϵ$^{l(3)j2B10}$, hsleoII^{L}	HS	100	100[a]	425
D14-3-3ϵ^{ex4}/D14-3-3ϵ^{ex4}	18°	42	—	382
D14-3-3ϵ^{ex4}/D14-3-3ϵ^{ex4}	23°	45	5.5	411
D14-3-3ϵ^{ex4}/D14-3-3ϵ^{ex4}	HS	45	5.5	409
D14-3-3ϵ^{ex4}/D14-3-3ϵ^{ex4}, hsleoI^{L}	18°	49	—	481
D14-3-3ϵ^{ex4}/D14-3-3ϵ^{ex4}, hsleoI^{L}	23°	56	14	440
D14-3-3ϵ^{ex4}/D14-3-3ϵ^{ex4}, hsleoI^{L}	HS	87	74.5[a]	493
D14-3-3ϵ^{ex4}/D14-3-3ϵ^{ex4}, hsleoI^{H}	18°	51	—	415
D14-3-3ϵ^{ex4}/D14-3-3ϵ^{ex4}, hsleoI^{H}	23°	60	18.5	433
D14-3-3ϵ^{ex4}/D14-3-3ϵ^{ex4}, hsleoI^{H}	HS	85	69[a]	495
D14-3-3ϵ^{ex4}/D14-3-3ϵ^{ex4}, hsleoII^{L}	18°	49	—	496
D14-3-3ϵ^{ex4}/D14-3-3ϵ^{ex4}, hsleoII^{L}	23°	69	39[a]	534
D14-3-3ϵ^{ex4}/D14-3-3ϵ^{ex4}, hsleoII^{L}	HS	100	100[a]	555
D14-3-3ϵ^{ex4}/D14-3-3ϵ^{ex4}, hsleoII^{H}	18°	56	—	512
D14-3-3ϵ^{ex4}/D14-3-3ϵ^{ex4}, hsleoII^{H}	23°	91	76.5[a]	534
D14-3-3ϵ^{ex4}/D14-3-3ϵ^{ex4}, hsleoII^{H}	HS	100	100[a]	485
D14-3-3ϵ^{ex4}/D14-3-3ϵ^{ex4},UASleoI	25°	37	—	230
elavGal4/+ ; D14-3-3ϵ^{ex4}/D14-3-3ϵ^{ex4},UASleoI	25°	63	41[a]	331
D14-3-3ϵ^{ex4}/D14-3-3ϵ^{ex4},UASleoII	25°	34	—	248
elavGal4/+; D14-3-3ϵ^{ex4}/D14-3-3ϵ^{ex4},UASleoII	25°	100	100[a]	380

leo transgenes rescue the lethality of *D14-3-3ϵ* mutant homozygotes. The temperature conditions employed for the crosses are shown under "Temperature." Under HS conditions, flies were raised under constant 23°, except for three daily 30-min, 32° heat shocks. Viability was calculated as the fraction of adults of each genotype recovered from crosses of balanced individuals over that expected if the mutant homozygotes were fully viable. "% rescue" was calculated as the increase in mutant homozygotes carrying transgenes over the "baseline" number (—). The superscripts *H* and *L* for *leoI* and *leoII* transgenes denote high- and low-expressing transgenes, respectively. *n* denotes the total number of flies scored per cross that yielded the mutant homozygotes carrying *D14-3-3ϵ* or *leo* transgenes.

[a] Significant rescue.

for the strong hypomorphic transposon insertion allele *leo^{P1188}* die as fully formed larvae, while the null *leo^{12X}* homozygotes exhibit deficits on their dorsal side including incomplete closure (Skoulakis and Davis 1996; Broadie *et al.* 1997). Semiquantitative Western blot analysis indicated that the level of D14-3-3ϵ remained relatively unchanged in homozygous *leo^{P1188}* and *leo^{12X}* mutant embryos in comparison to their heterozygous siblings (Figure 5). LEO elevation was again readily detectable in *D14-3-3ϵ^{ex4}* homozygotes. Therefore, we could not detect reciprocal elevation of D14-3-3ϵ upon loss of LEO in embryos.

The level of LEO is unchanged in *D14-3-3ϵ* adult heads: Does LEO remain elevated in adult *D14-3-3ϵ* mutant homozygotes? Is D14-3-3ϵ elevated in adult *leo* mutant heterozygotes? To address these questions, we determined the relative levels of LEO in isolated heads of *D14-3-3ϵ^{ex4}* homozygotes and heterozygotes and of D14-3-3ϵ in *leo* mutant heterozygotes because both proteins are enriched in adult brains (Skoulakis and Davis 1996; S. F. Acevedo, unpublished observations). Although the 50% reduction of D14-3-3ϵ in *D14-3-3ϵ^{ex4}* heterozygotes and *leo^{1188}/+; D14-3-3ϵ^{ex4}/+* animals was readily detectable, LEO levels in *D14-3-3ϵ^{ex4}* homozygotes were not significantly different from *D14-3-3ϵ^{ex5}* (Student's *t*-tests, $P = 0.8678$) or from *w^{1118}* controls (Figure 6). Similar results were obtained for *D14-3-3ϵ$^{l(3)j2B10}$* homozygotes (supplemental Figure 2 at http://www.genetics.org/supplemental/). Thus, LEO appears to be elevated only in *D14-3-3ϵ* mutant embryos around

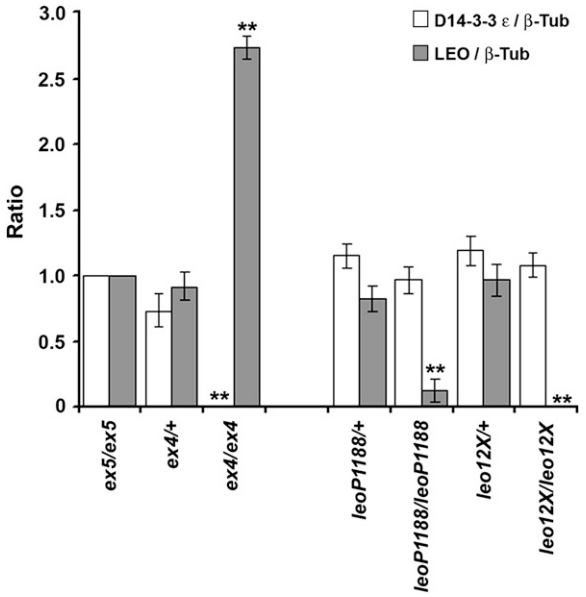

FIGURE 5.—D14-3-3ϵ is not elevated in *leo* homozygous mutant embryos. The average ratios (±SEM) of LEO/β-TUB and D14-3-3ϵ/β-TUB are shown from three individual experiments. Ratios are shown relative to those obtained from *D14-3-3ϵ*^{ex5}/*D14-3-3ϵ*^{ex5} embryos, which were arbitrarily set to 1. The genotypes of the embryos whose lysates were blotted are *ex5/ex5* for *D14-3-3ϵ*^{ex5}/*D14-3-3ϵ*^{ex5}; *ex4/+* for *D14-3-3ϵ*^{ex4}/*D14-3-3ϵ*^{ex5}; *ex4/ex4* for *D14-3-3ϵ*^{ex4}/*D14-3-3ϵ*^{ex4}, whereas full genotypes are shown for *leo* mutants. Compared to that in *D14-3-3ϵ*^{ex5} homozygotes, the level of LEO accumulation was significantly higher (**$P < 0.001$) in *D14-3-3ϵ*^{ex4} homozygotes and significantly reduced (**$P < 0.001$) in *leo*^{1188} homozygotes. The level of D14-3-3ϵ was also significantly reduced in late *D14-3-3ϵ*^{ex4} homozygous embryos.

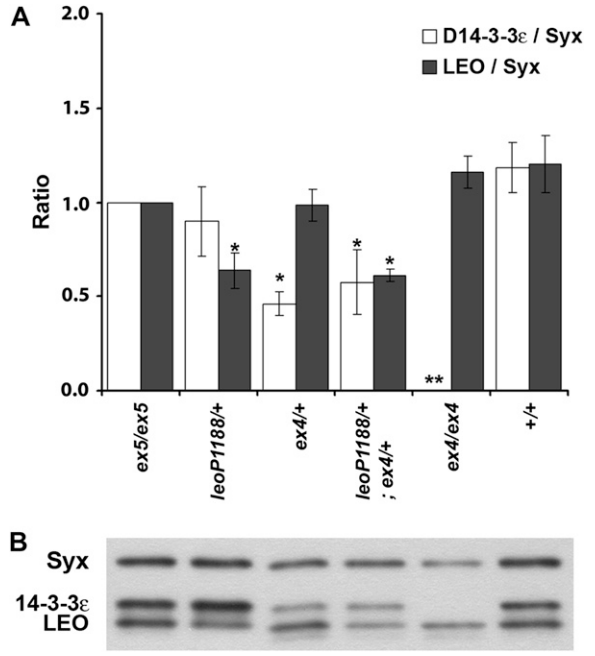

FIGURE 6.—LEO is not significantly elevated in the heads of adult *D14-3-3ϵ* homozygous mutants, and the level of D14-3-3ϵ is not changed in the heads of *leo* mutant heterozygotes. (A) The average ratios (±SEM) of LEO/SYX and D14-3-3ϵ/SYX is shown from three individual Western blotting experiments, one of which is shown in B. Ratios are shown relative to those obtained from *D14-3-3ϵ*^{ex5}/*D14-3-3ϵ*^{ex5} adults, which were arbitrarily set to 1. Compared to the levels in *D14-3-3ϵ*^{ex5}/*D14-3-3ϵ*^{ex5} controls, D14-3-3ϵ was significantly reduced (*$P < 0.01$) in *D14-3-3ϵ*^{ex4}/*D14-3-3ϵ*^{ex5} (*ex4/+*), *leo*^{P1188}*/+; D14-3-3ϵ*^{ex4}*/+* (*leoP1188/+; ex4/+*) double heterozygotes and *D14-3-3ϵ*^{ex4}/*D14-3-3ϵ*^{ex4} (*ex4/ex4*) homozygotes (**$P < 0.001$). Similarly, LEO was significantly (*$P < 0.01$) reduced in *leo*^{P1188}*/+* and *leo*^{P1188}*/+; D14-3-3ϵ*^{ex4}*/+* animals. However, LEO was not significantly elevated in the heads of *D14-3-3ϵ*^{ex4} homozygotes or D14-3-3ϵ in the heads of *leo*^{P1188} heterozygotes. (B). A representative blot of head lysates from the indicated genotypes quantified in A. The neuronal protein SYNTAXIN (Syx) was utilized to normalize the amount of each lysate loaded.

the time of hatching, and therefore it is unlikely that it functionally compensates for D14-3-3ϵ loss in all tissues. Similarly, D14-3-3ϵ is not elevated in the heads of *leo* mutant heterozygotes.

Loss of D14-3-3ϵ disrupts wing cross-vein formation: Adult *D14-3-3ϵ*^{ex4} and *D14-3-3ϵ*$^{l(3)j2B10}$ homozygotes have smaller wings than control flies. Cell counts along the longitudinal veins of homozygous and heteroallelic adults indicated a 10% proportional reduction in length compared to *D14-3-3ϵ*^{ex5} controls (not shown). This may be a consequence of the overall body-size reduction also observed in null homozygous and heteroallelic embryos (Figure 2), larvae, and adults. In addition, the majority of adult *D14-3-3ϵ*^{ex4} and *D14-3-3ϵ*$^{l(3)j2B10}$ homozygotes exhibited a conspicuous lack of the dorsal part of the posterior cross-vein and, with lesser penetrance, malformation of the anterior cross-vein (Figure 7, A.2–A.5). These defects map to *D14-3-3ϵ*, as all mutant animals exhibited the phenotype (Table 5A). Furthermore, posterior and anterior cross-vein deficits can be rescued with *hsD14-3-3ϵ* transgenes (Figure 7, A.6 and A.7; Table 5B), demonstrating that cross-vein formation indeed requires D14-3-3ϵ. We quantified deficits of the posterior cross vein because it exhibited greater penetrance and therefore afforded more sensitivity to rescue experiments and is reported on the "% rescue" column in Table 5, B and C. Significant changes in the fraction of wings that exhibited anterior cross-vein malformations are denoted by footnote *a* in Table 5.

Overexpression of *leoI* partially rescues the wing-venation deficits of *D14-3-3ϵ* mutants: Can LEO compensate for the D14-3-3ϵ requirement in cross-vein formation as it did for hatching? *leoI*, but not *leoII*, is expressed in wing disks (Figure 7B), whereas transcripts for both isoforms could be detected in brains from the same *w*^{1118} larvae as reported previously (PHILIP *et al.* 2001). To determine whether LEO compensates D14-3-3ϵ loss in wing cross-vein formation, we examined the wings of *D14-3-3ϵ*^{ex4} homozygotes rescued from lethality by *hsleoI* and *hsleoII* transgenes. Both *hsleoI* and *hsleoII* transgenes were expressed in the wing disks after heat

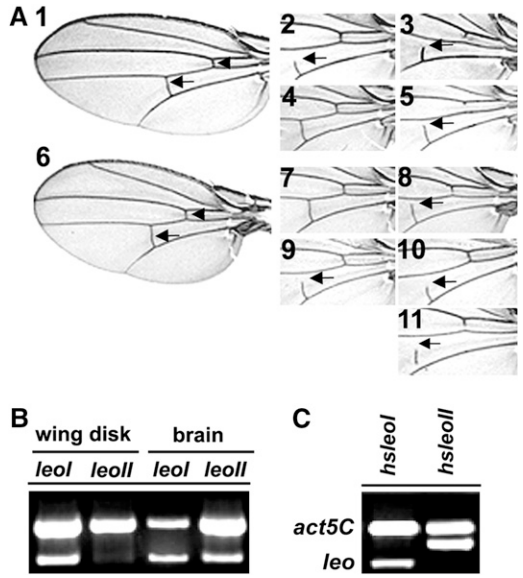

FIGURE 7.—Deficits in cross-vein formation of *D14-3-3ϵ* mutants and transgenic rescue by *D14-3-3ϵ* and *leo* transgenes. (A) Posterior cross veins are indicated by arrows, while anterior cross veins are indicated by arrowheads in 1 and 6. Genotypes are 1, $D14\text{-}3\text{-}3\epsilon^{ex5}/D14\text{-}3\text{-}3\epsilon^{ex5}$; 2, $D14\text{-}3\text{-}3\epsilon^{l(3)j2B10}/D14\text{-}3\text{-}3\epsilon^{l(3)j2B10}$; 3, $D14\text{-}3\text{-}3\epsilon^{ex4}/D14\text{-}3\text{-}3\epsilon^{ex4}$; 4, $D14\text{-}3\text{-}3\epsilon^{ex4}/D14\text{-}3\text{-}3\epsilon^{ex5}$; 5, $D14\text{-}3\text{-}3\epsilon^{l(3)j2B10}/D14\text{-}3\text{-}3\epsilon^{ex4}$ heteroallelic, exhibiting anterior cross-vein deficits also; 6, $D14\text{-}3\text{-}3\epsilon^{ex4}/D14\text{-}3\text{-}3\epsilon^{ex4}$, *hsD14-3-3ϵ* raised under HS conditions; 7, $D14\text{-}3\text{-}3\epsilon^{l(3)j2B10}/D14\text{-}3\text{-}3\epsilon^{l(3)j2B10}$, *hsD14-3-3ϵ* raised under HS conditions; 8, $D14\text{-}3\text{-}3\epsilon^{ex4}/D14\text{-}3\text{-}3\epsilon^{ex4}$, *hsD14-3-3ϵ* raised at 18°; 9, $D14\text{-}3\text{-}3\epsilon^{ex4}/D14\text{-}3\text{-}3\epsilon^{ex4}$, *hsleoI* raised under HS conditions; 10, $D14\text{-}3\text{-}3\epsilon^{ex4}/D14\text{-}3\text{-}3\epsilon^{ex4}$, *hsleoII* raised under HS conditions; 11, A $D14\text{-}3\text{-}3\epsilon^{ex4}/D14\text{-}3\text{-}3\epsilon^{ex4}$, *hsleoII* raised under HS conditions where both anterior and posterior cross veins remained defective. (B) Products of a RT–PCR experiment with RNA from larval wing disks and brains with primers specific for *leoI* and *leoII* transcripts (bottom) and amplification of *act5C* transcripts (top amplicon) as controls for the quality of the transcription. *leoII* is not expressed in larval wing disks. (C) Products of RT–PCR with transgene-specific primers (PHILIP *et al.* 2001), indicating that under HS conditions both *leoI* and *leoII* transgenes are expressed in dissected wing disks.

shock (Figure 7C). However, although *hsleoII* is efficient at rescuing lethality, the wings of the same rescued mutant homozygotes retained the posterior cross-vein deficit (Figure 7A.10) and often the anterior cross-vein remained malformed (Figure 7A.11). In contrast, a 25% reduction in posterior cross-vein deficits and a complete rescue of anterior cross-vein malformation was observed in animals rescued from lethality with *hsleoI* transgenes (Table 5). Similar results were obtained with $D14\text{-}3\text{-}3\epsilon^{l(3)j2B10}$ homozygotes expressing *hsleoI* and *hsleoII* transgenes (not shown). These data indicate that LEOI and D14-3-3ϵ are partially redundant in processes required for posterior cross-vein formation. Moreover, LEOII is much more inefficient in compensating D14-3-3ϵ loss in anterior cross-vein formation. Therefore, the two LEO isoforms again are not equivalent in their ability to substitute for the loss of D14-3-3ϵ.

DISCUSSION

***D14-3-3ϵ* is an essential gene:** Our results utilizing null alleles indicate that *D14-3-3ϵ* is not dispensable for viability, but its loss is partially compensated by elevation of endogenous *leo* levels. Consequently, homozygotes survive to adulthood, whose number is higher when the hypomorphic allele $D14\text{-}3\text{-}3\epsilon^{l(3)j2B10}$ is used. This is the likely reason for the suggestion of previous reports that the gene is not essential (CHANG and RUBIN 1997; BENTON *et al.* 2002). This interaction is uncovered genetically by the inability to obtain $D14\text{-}3\text{-}3\epsilon^{ex4}$ and $D14\text{-}3\text{-}3\epsilon^{l(3)j2B10}$ homozygotes when one copy of *leo* is mutated (*i.e.*, $leo^{P1188}/+$; $D14\text{-}3\text{-}3\epsilon^{l(3)j2B10}/D14\text{-}3\text{-}3\epsilon^{l(3)j2B10}$ animals). Embryos homozygous for mutant alleles do not exhibit obvious morphological defects (Figure 2) because maternally provided D14-3-3ϵ is likely sufficient to fulfill its requirement in syncytial cellular blastoderm and gastrulating animals (TIEN *et al.* 1999; PHILIP *et al.* 2001; SU *et al.* 2001). *D14-3-3ϵ* mutant homozygotes die ostensibly because lack of zygotic protein from the nervous system renders them unable to hatch. Similarly, LEO accumulates in embryonic motor neurons innervating the body-wall musculature and its loss in *leo* mutants is the likely reason for their failure to hatch despite their apparently normal progression through development (BROADIE *et al.* 1997).

14-3-3 homeostasis: Our results demonstrate that LEOII overaccumulates in late *D14-3-3ϵ* null embryos and that this elevation allows a fraction of them to hatch and survive. The conclusion is supported by the striking increase in the number of *D14-3-3ϵ* mutant homozygotes that survive upon expression of *leoII* transgenes in the nervous system (Table 4). Because endogenous LEOII accumulates preferentially in the CNS (BROADIE *et al.* 1997; PHILIP *et al.* 2001), our data suggest that its elevation in this tissue leads to successful hatching and survival of *D14-3-3ϵ* mutant homozygotes. This "homeostatic" response in *D14-3-3ϵ* mutants is specific to late embryogenesis after the maternally supplied D14-3-3ϵ, which perdures almost until stage 8 (S. F. ACEVEDO and K. TSIGKARI, unpublished results), has decayed. Therefore, the response appears specific to a period when the overall level of either 14-3-3's or D14-3-3ϵ, specifically, is critically important for survival.

It appears that a mechanism sensing the absence of D14-3-3ϵ operates in embryos and responds by increasing the level of LEOII. Congruent with this, LEO elevation was not observed in embryos homozygous for the dominant-negative allele $D14\text{-}3\text{-}3\epsilon^{E183K}$ (CHANG and RUBIN 1997), which compromises D14-3-3ϵ functionally, but does not change its overall levels in the embryo (supplemental Table 1 at http://www.genetics.org/supplemental/). It is possible that this is the reason that $D14\text{-}3\text{-}3\epsilon^{E183K}$ homozygotes are never recovered. Furthermore, this response appears specific to the loss of D14-3-3ϵ, because levels of this protein remained

TABLE 5

Wing cross-vein deficits of *D14-3-3ϵ* mutants and transgenic rescue

Genotype	% anterior malformed	% posterior malformed	% rescue
A.			
D14-3-3ϵ^{ex5}/D14-3-3ϵ^{ex5}	0	0	—
D14-3-3ϵ^{ex5}/D14-3-3ϵ$^{l(3)j2B10}$	0	0	—
D14-3-3ϵ^{ex5}/D14-3-3ϵ^{ex4}	0	0	—
D14-3-3ϵ$^{l(3)j2B10}$/D14-3-3ϵ$^{l(3)j2B10}$	25.0	75.0	—
D14-3-3ϵ$^{l(3)j2B10}$/D14-3-3ϵ^{ex4}	26.7	82.4	—
D14-3-3ϵ^{ex4}/D14-3-3ϵ^{ex4}	42.9	80.9	—
B.			
D14-3-3ϵ^{ex4}/D14-3-3ϵ^{ex4}, hsD14-3-3ϵ^{L} (18°)	40.6	83	—
D14-3-3ϵ^{ex4}/D14-3-3ϵ^{ex4}, hsD14-3-3ϵ^{L}	9.3[a]	14[a]	82.3
D14-3-3ϵ^{ex4}/D14-3-3ϵ^{ex4}, hsD14-3-3ϵ^{H} (18°)	41.8	79.5	—
D14-3-3ϵ^{ex4}/D14-3-3ϵ^{ex4}, hsD14-3-3ϵ^{H}	0[a]	3.6[a]	95.6
C.			
D14-3-3ϵ^{ex4}/D14-3-3ϵ^{ex4}, hsleoI^{L} (18°)	43.2	82.2	—
D14-3-3ϵ^{ex4}/D14-3-3ϵ^{ex4}, hsleoI^{L}	29[a]	72	11
D14-3-3ϵ^{ex4}/D14-3-3ϵ^{ex4}, hsleoI^{H} (18°)	41.3	80.9	—
D14-3-3ϵ^{ex4}/D14-3-3ϵ^{ex4}, hsleoI^{H}	0[a]	60	25.8
D14-3-3ϵ^{ex4}/D14-3-3ϵ^{ex4}, hsleoII^{L} (18°)	43.4	82.6	—
D14-3-3ϵ^{ex4}/D14-3-3ϵ^{ex4}, hsleoII^{L}	40	78.4	3.1
D14-3-3ϵ^{ex4}/D14-3-3ϵ^{ex4}, hsleoII^{H} (18°)	41.5	81.8	—
D14-3-3ϵ^{ex4}/D14-3-3ϵ^{ex4}, hsleoII^{H}	33	76.8	5.1

The wing cross-vein deficits are rescued by conditional *hsD14-3-3ϵ* expression, but not by *leo* transgenes. (A) Percentage of *D14-3-3ϵ* controls and mutant homozygotes that exhibited posterior and anterior cross-vein deficits. Posterior and anterior cross-vein deficits were counted on the same wings and one wing was scored per individual ($n > 100$). (B) The percentage of *D14-3-3ϵ^{ex4}/D14-3-3ϵ^{ex4}, hsD14-3-3ϵ* exhibiting wing cross-vein deficits raised under conditions of transgene silence (18°) or induction. The "% rescue" indicates the percentage decrease in individuals with deficient wings and is shown only for posterior cross veins. (C). The percentage of *D14-3-3ϵ^{ex4}/D14-3-3ϵ^{ex4}* individuals expressing *leoI* and *leoII* transgenes exhibiting wing cross-vein deficits raised under conditions of transgene silence (18°) or induction. The "% rescue" indicates the percentage decrease in individuals with deficient wings and is shown only for posterior cross veins.

[a] Large changes in the percentage of deficient wings (rescue).

normal in homozygous *leo* mutant embryos and adults (Figures 4 and 5), consistent with their strong lethal phenotype. Clearly, this sensing mechanism responds by increased accumulation of *leoII* transcripts by preferential utilization of one of two possible promoters and splicing of the primary transcript to include the *leoII*-specific exon 6′ (Kockel *et al.* 1997; Philip *et al.* 2001). How is lack of D14-3-3ϵ sensed and how could *leoII* transcription be increased? 14-3-3's have been reported to participate in nuclear/cytoplasmic trafficking of transcription factors (Brunet *et al.* 2002; Zhao *et al.* 2004; Berdichevsky and Guarente 2006). Therefore, it is possible that loss of D14-3-3ϵ enhances transcription from the proximal promoter of the *leo* gene by not mediating nuclear export of a factor that binds that site. Alternatively, D14-3-3ϵ may be part of a repressing complex and, upon its loss, transcription from this site is enhanced. In contrast, excessive transgenic elevation in the amount of D14-3-3ϵ results in recovery of few adults (<10% of expected) homozygous for strong hypomorphic *leo* mutations (K. Tsigkari and E. M. C. Skoulakis, unpublished results). This suggests that although D14-3-3ϵ can at least partially compensate for the loss of LEO in high concentrations, an endogenous molecular mechanism to elevate it in *leo* homozygotes does not appear to exist.

Although *leoI* transcripts accumulate in the wing disk, LEO does not appear to play a role in wing-vein formation because animals that develop with as low as 10% of normal LEO do not exhibit wing aberrations (Philip *et al.* 2001). Therefore, the venation deficits are a phenotype specific to *D14-3-3ϵ* mutant homozygotes. Interestingly, in congruence with the mechanism proposed above, the *leoI* transcripts normally expressed in that tissue were not upregulated and *leoII* transcripts were not ectopically transcribed in *D14-3-3ϵ* mutant homozygote wing disks (S. F. Acevedo, unpublished observations). This is because the proposed D14-3-3ϵ-interacting factor(s) required for exon 1′-containing *leoII* transcription are likely absent from the wing disk where these transcripts do not normally accumulate. Exon 1-containing *leoII* transcripts do not appear to require such D14-3-3ϵ-interacting factor(s), since these transcripts were not upregulated in embryos. Therefore, loss of D14-3-3ϵ does

not alter the tissue specificity of *leo* transcriptional regulation and specific isoform accumulation.

It is presently unclear whether this compensatory mechanism is operant in other systems where mutant analyses of 14-3-3's have been initiated. Interestingly, single nulls of either 14-3-3-encoding gene in *Saccharomyces cerevisiae* are viable, while the double mutant is lethal (Roberts *et al.* 1997) and similar results were obtained for the two *Schizosaccharomyces pombe* genes (Ford *et al.* 1994). These observations may reflect similar 14-3-3 "homeostatic" mechanisms in these species. Directed reduction of specific 14-3-3 protein levels during *Xenopus laevis* development yielded gastrulation and patterning defects for all proteins tested except for 14-3-3ζ (Lau *et al.* 2006). Unlike Drosophila, Xenopus 14-3-3ζ may not be essential for development, but it is also possible that loss of this isotype is specifically compensated for by elevation of the remaining 14-3-3's. Such mechanisms, if extant in mammals, are likely to hinder genetic analysis of 14-3-3 function, especially in the brain where all family members are expressed (Baxter *et al.* 2002). Interestingly, mice mutant for 14-3-3ϵ exhibit severe brain abnormalities and die perinatally, yet a small fraction survive to adulthood appearing smaller, but otherwise normal (Toyo-oka *et al.* 2003), much like the Drosophila mutants. It is unknown whether 14-3-3ζ or other isotypes are elevated in these animals as predicted by our results.

Functional specificity and redundancy of 14-3-3's: Functional specificity of 14-3-3 family members may be the result of tissue or temporal-specific gene expression and regulation or of isotype-specific ligand selectivity. Isotypes may have redundant functions within a cell if they are able to interact with the same targets. Even then, affinity differences toward common ligands predicted by their amino-acid sequence and tertiary structure (Gardino *et al.* 2006) may functionally differentiate coexpressed 14-3-3's.

Although both *leoI* and *leoII* transgenes rescued the lethality of *D14-3-3ϵ* mutants, they clearly exhibited different efficiency (Table 4). Rescue was invariably higher upon accumulation of LEOII either ubiquitously or specifically in the nervous system. However, rescue required excessive accumulation of LEOII to overcome loss of D14-3-3ϵ. In fact, the two- to threefold LEO elevation shown in Figure 3B could be as much as a 50–60% underestimate of the level of this protein in *D14-3-3ϵ* mutant embryos that hatch. Therefore, a large excess of LEO appears to be necessary to functionally substitute D14-3-3ϵ in the embryonic nervous system, which may be attained only in a small number of mutant homozygotes. This probably reflects the affinity differences that LEO dimers exhibit toward client proteins normally bound either by D14-3-3ϵ homodimers or by D14-3-3ϵ/LEO heterodimers. If so, then even a small amount of D14-3-3ϵ would increase the number of mutant homozygotes obtained. In agreement with this, more homozygotes were recovered from the transposon allele *D14-3-3ϵ*$^{l(3)j2B10}$, which likely contains residual D14-3-3ϵ (Table 1). Differences in ligand binding between LEOI and LEOII are likely reflected in the large difference with which the two isoforms rescue the lethality of *D14-3-3ϵ* mutants. This is the first unequivocal demonstration of functional differences between LEOI and LEOII. These differences must reside in the five unique amino acids of helix 6 that distinguish the two isoforms (Philip *et al.* 2001). It is unknown whether LEOI, LEOII, or both contribute to the reported redundancy with D14-3-3ϵ in photoreceptor development and oocyte polarity (Chang and Rubin 1997; Benton *et al.* 2002; Benton and St Johnston 2003).

Interestingly, the functional redundancy of LEO isoforms with D14-3-3ϵ is tissue specific. In contrast to the embryonic nervous system, enhanced accumulation of LEOI, and not of LEOII, was able to compensate for anterior cross-vein deficits and partially for the posterior cross vein (Table 5). Again, this suggests that D14-3-3ϵ ligands in the wing disk necessary for cross-vein formation can be targeted by excess LEOI (and not LEOII). Hence, LEOII can be redundant with D14-3-3ϵ specifically in the embryonic nervous system where it is presumed to accumulate preferentially, while in the wing disk LEOI, which is normally found in this tissue, is the potential compensating isoform. Similarly, although the two *S. cerevisiae* 14-3-3 genes are functionally redundant for viability, only one, *Bmh1p*, is required for efficient forward transport to the endoplasmic reticulum (Michelsen *et al.* 2006). Thus, redundancy of 14-3-3's largely depends on the specific function and interacting proteins that they engage within a particular tissue or developmental context.

Collectively, our data show a tissue- and temporal-specific upregulation of *leo* transcription that can account for the apparent functional redundancy between LEO and D14-3-3ϵ with respect to the lethality of *D14-3-3ϵ* mutants and possibly other processes requiring these proteins. In addition, this analysis for the first time demonstrates tissue and temporal functional differences between the two LEO isoforms. Whether these functional differences and the functional redundancy among the Drosophila 14-3-3's will also occur in the adult nervous system where they are all most abundant is currently unknown. A previous study failed to uncover differences between LEOI and LEOII with respect to learning and memory (Philip *et al.* 2001). Nevertheless, our data strongly support the notion that the existence of multiple 14-3-3 isotypes in metazoans reflects a combination of tissue- and temporal-specific isotype expression, localization, and functional specialization. Importantly, this analysis indicates that understanding the biological roles of 14-3-3's will require identification of proteins engaged by homo- and heterodimers of particular composition in a tissue- and temporal-specific manner.

The authors are indebted to H. Chang and G. Rubin for providing mutant stocks and plasmids, to C.-T. Chien for providing an anti-D14-3-3ϵ antibody used in initial phases of this work, to Charity Moore for

help with analysis of the wing phenotype, to Mary McCrady, Courtney Swayze, Alexandros Kanellopoulos, and Maria Anezaki for stock maintenance and husbandry, and to M. Franco-Redrejo for invaluable help with quantitative RT–PCR. We thank Hanh Nguyen for anti-MEF2 antibodies, the Developmental Hybridoma Studies Bank at the University of Iowa (Iowa City, IA) for monoclonal antibodies, and Terry Orr-Weaver and Sumana Datta for valuable discussions and suggestions. This work was supported by a European Commission Marie Curie grant (IRG-003570), by PENED (01EΔ207) from the Greek General Secretariat for Research and Technology, and by the National Science Foundation (grant IBN-0080687).

LITERATURE CITED

Aitken, A., 1995 14–3-3 proteins on the MAP. Trends Biochem. Sci. **20:** 95–97.

Aitken, A., S. Howell, D. Jones, J. Madrazo and Y. Patel, 1995 14–3-3 α and δ are the phosphorylated forms of Raf-activating 14–3-3 β and ζ. J. Biol. Chem. **270:** 5706–5709.

Aitken, A., H. Baxter, T. Dubios, S. Clokie, S. Mackie *et al.*, 2002 14–3-3 proteins in cell regulation. Biochem. Soc. Trans. **30:** 351–360.

Baxter, H. C., W.-G. Liu, J. L. Forster, A. Aitken and J. R. Fraser, 2002 Immunolocalisation of 14–3-3 isoforms in normal and scrapie-infected murine brain. Neuroscience **109:** 5–14.

Benton, R., and D. St Johnston, 2003 Drosophila PAR-1 and 14–3-3 inhibit Bazooka/PAR-3 to establish complementary cortical domains in polarized cells. Cell **115:** 691–704.

Benton, R., I. M. Palacios and D. St. Johnston, 2002 *Drosophila* 14–3-3/PAR-5 is an essential mediator of PAR1 function in axis formation. Dev. Cell **3:** 659–671.

Berdichevsky, A., and L. Guarente, 2006 A stress response pathway involving sirtuins, forkheads and 14–3-3 proteins. Cell Cycle **5:** 2588–2591.

Bourgouin, C., S. E. Lundgren and J. B. Thomas, 1992 Apterous is a Drosophila LIM domain gene required for the development of a subset of embryonic muscles. Neuron **9:** 549–561.

Brand, A. H., and N. Perrimon, 1993 Targeted gene expression as a means of altering cell fates and generating dominant phenotypes. Development **118:** 401–415.

Bridges, D., and G. B. G. Moorehead, 2005 14–3-3 proteins: a number of functions for a numbered protein. Sci. STKE **2005:** re10.

Broadie, K., E. Rushton, E. M. C. Skoulakis and R. L. Davis, 1997 Leonardo, a Drosophila 14–3-3 protein involved in learning, regulates presynaptic function. Neuron **19:** 391–402.

Brunet, A., F. Kanai, J. Stehn, J. Xu, D. Sarbassova *et al.*, 2002 14–3-3 transits to the nucleus and participates in dynamic nucleocytoplasmic transport. J. Cell Biol. **156:** 817–828.

Chang, H. C., and G. M. Rubin, 1997 14–3-3ϵ positively regulates Ras mediated signaling in Drosophila. Genes Dev. **11:** 1132–1139.

Chen, H.-K., P. Fernandez-Funez, S. F. Acevedo, Y. C. Lam, M. D. Kaytor *et al.*, 2003 Interaction of akt-phosphorylated ataxin-1 with 14–3-3 mediates neurodegeneration in spinocerebellar ataxia type 1. Cell **113:** 457–468.

Coblitz, B., M. Wu, S. Shikano and M. Li, 2006 C-terminal binding: an expanded repertoire and function of 14–3-3 proteins. FEBS Lett. **580:** 1531–1535.

Ford, J. C., F. al-Khodairy, E. Fotou, K. S. Sheldrick, D. J. Griffiths *et al.*, 1994 14–3-3 protein homologs required for the DNA damage checkpoint in fission yeast. Science **265:** 533–535.

Foundoulakis, M., R. Hardmeier, H. Hoger and G. Lubec, 2001 Postmortem changes in the level of brain proteins. Exp. Neurol. **167:** 86–94.

Fu, H., R. R. Subramanian and S. C. Masters, 2000 14–3-3 proteins: structure, function and regulation. Annu. Rev. Pharmacol. Toxicol. **40:** 617–647.

Gardino, A. K., S. J. Smerdon and M. B. Yaffe, 2006 Structural determinants of 14–3-3 binding specificities and regulation of subcellular localization of 14–3-3-ligand complexes: a comparison of the X-ray crystal structures of all human 14–3-3 isoforms. Semin. Cancer Biol. **16:** 173–182.

Jones, D. H. A., H. Martin, J. Madrazo, K. A. Robinson, P. Neilsen *et al.*, 1995 Expression and structural analysis of 14–3-3 proteins. J. Mol. Biol. **245:** 375–384.

Karim, F. D., H. C. Chang, M. Therrien, D. A. Wassarman, T. Laverty *et al.*, 1996 A screen for genes that function downstream of Ras1 during Drosophila eye development. Genetics **143:** 315–329.

Kockel, L., G. Vorbraggen, H. Jackle, M. Mlodzik and D. Bohnmann, 1997 Requirement for Drosophila 14–3-3 ζ in cell proliferation and Raf-dependent photoreceptor development. Genes Dev. **11:** 1140–1147.

Lau, J. M., C. Wu and A. J. Muslin, 2006 Differential role of 14–3-3 family members in Xenopus development. Dev. Dyn. **235:** 1761–1776.

Li, W., E. M. C. Skoulakis, R. L. Davis and N. Perrimon, 1997 The Drosophila 14–3-3 protein Leonardo enhances Torso signaling through D-Raf in a Ras1-dependent manner. Development **124:** 4163–4171.

Li, W., E. Noll and N. Perrimon, 2000 Identification of autosomal regions involved in Drosophila Raf function. Genetics **156:** 763–774.

Luo, Z., X. Zhang, U. Rapp and J. Avruch, 1995 Identification of the 14–3-3ζ domains important for self-association and Raf binding. J. Biol. Chem. **270:** 23681–23687.

Martin, H., J. Rostas, Y. Patel and A. Aitken, 1994 Subcellular localisation of 14–3-3 isoforms in rat brain using specific antibodies. J. Neurochem. **63:** 2259–2265.

Michelsen, K., T. Mrowiec, K. E. Duderstadt, S. Frey, D. L. Minor *et al.*, 2006 A multimeric membrane protein reveals 14–3-3 isoform specificity in forward transport in yeast. Traffic **7:** 903–916.

Muslin, A. J., J. W. Tanner, P. M. Allen and A. S. Shaw, 1996 Interaction of 14–3-3 with signaling proteins is mediated by the recognition of phosphoserine. Cell **84:** 889–897.

Nguyen, H. T., and X. Xu, 1998 Drosophila *mef2* expression during mesoderm development is controlled by a complex array of *cis*-acting regulatory modules. Dev. Biol. **204:** 550–566.

Pfaffl, M. W., 2001 A new mathematical model for relative quantification in real-time RT-PCR. Nucleic Acids Res. **29:** 2002–2007.

Philip, N., S. Acevedo and E. M. C. Skoulakis, 2001 Conditional rescue of olfactory learning and memory defects in mutants of the 14–3-3ζ gene *leonardo*. J. Neurosci. **21:** 8417–8425.

Roberts, R. L., H. U. Mosch and G. R. Fink, 1997 14–3-3 proteins are essential for RAS/MAPK cascade signaling during pseudohyphal development in *S. cerevisiae*. Cell **89:** 1055–1065.

Robinow, S., and K. White, 1988 The locus elav of *Drosophila melanogaster* is expressed in neurons at all developmental stages. Dev. Biol. **126:** 294–303.

Rosenquist, M., P. Sehnke, R. J. Ferl, M. Sommarin and C. Larsson, 2000 Evolution of the 14–3-3 protein family: Does the large number of isoforms in multicellular organisms reflect functional specificity? J. Mol. Evol. **51:** 446–458.

Skoulakis, E. M. C., and R. L. Davis, 1996 Olfactory learning deficits in mutants for leonardo, a Drosophila gene encoding a 14–3-3 protein. Neuron **17:** 931–944.

Skoulakis, E. M. C., and R. L. Davis, 1998 14–3-3 proteins in neuronal development and function. Mol. Neurobiol. **16:** 269–284.

Su, T. T., D. H. Parry, B. Donahoe, C.-T. Chien, P. H. O'Farrell *et al.*, 2001 Cell cycle roles for the two 14–3-3 proteins during *Drosophila* development. J. Cell Sci. **114:** 3445–3462.

Tien, A.-C., H.-Y. Hsei and C.-T. Chien, 1999 Dynamic expression and cellular localization of the *Drosophila* 14–3-3e during embryonic development. Mech. Dev. **81:** 209–212.

Toyo-oka, K., A. Shionoya, M. J. Gambello, C. Cardoso, R. Leventer *et al.*, 2003 14–3-3epsilon is important for neuronal migration by binding to NUDEL: a molecular explanation for Miller-Dieker syndrome. Nat. Genet. **274:** 285.

Tzivion, G., and J. Avruch, 2002 14–3-3 proteins: active cofactors in cellular regulation by serine/threonine phosphorylation. J. Biol. Chem. **277:** 3061–3064.

Tzivion, G., Y. H. Shen and J. Zuh, 2001 14–3-3 proteins: bringing new definitions to scaffolding. Oncogene **20:** 6331–6338.

van Hemert, M. J., H. Y. Steensma and G. P. H. van Heudsen, 2001 14–3-3 proteins: key regulators of cell division, signalling and apoptosis. BioEssays **23:** 936–946.

van Heudsen, G. P. H., 2005 14–3-3 proteins: regulators of numerous eukaryotic proteins. IUBMB Life **57:** 623–629.

Wang, W., and D. Shakes, 1996 Molecular evolution of the 14–3-3 family. Mol. Evol. **43:** 384–398.

Wilker, E. W., R. A. Grant, S. C. Artim and M. B. Yaffe, 2005 A structural basis for 14–3-3sigma functional specificity. J. Biol. Chem. **280:** 18891–18898.

Xiao, B., S. Smerdon, D. H. Jones, G. G. Dodson, Y. Soneji *et al.*, 1995 Structure of a 14–3-3 protein and implications for coordination of multiple signalling pathways. Nature **376:** 188–191.

Yaffe, M. B., 2002 How do 14–3-3 proteins work? Gatekeeper phosphorylation and the molecular anvil hypothesis. FEBS Lett. **513:** 53–57.

Yaffe, M. B., and A. E. H. Elia, 2001 Phosphoserine/threonine-binding domains. Curr. Opin. Cell Biol. **13:** 131–138.

Zhao, X., L. Gan, H. Pan, D. Kan, M. Majeski *et al.*, 2004 Multiple elements regulate nuclear/cytoplasmic shuttling of FOXO1: characterization of phosphorylation- and 14–3-3-dependent and -independent mechanisms. Biochem. J. **378:** 839–849.

Communicating editor: W. M. Gelbart